Malaysian NANO-An International Journal

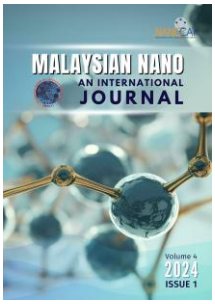

Research article

Synthesis of PMMA-PEG@TiO_2 Nanocomposite by Hydrothermal and Sol-Gel Techniques for Resveratrol Delivery

L. Jeswin Anto[a], J. Annaraj[a]* and Suresh Sagadevan[b]

[a]Department of Materials Science, School of Chemistry, Madurai Kamaraj University, Madurai-625 021, India
[b]Nanotechnology & Catalysis Research Centre, Institute of Advanced Studies, University of Malaya, 50603 Kuala Lumpur, Malaysia

Received 7th June 2024
Revised 14th June 2024
Accepted 28th June 2024

DOI:
10.22452/mnij.vol4no1.3

Corresponding authors:
annaraj.chem@mkuniversity.org

Abstract

TiO_2 nanoparticles were prepared using the sol-gel and hydrothermal procedures in order to compare their porosity, stability, and particle homogeneity as well as their encapsulation efficiency. Alcohol is converted into gel using the sol-gel method, which involves stirring it while it's hot, then drying, powdering, and calcining it. This simple process produces high-purity products, however due to agglomeration, it also produces unpredictable particle size and shape. On the other hand, hydrothermal approach requires enormous volumes at high pressure, which makes it slow and difficult to scale up. However, it is effective in producing uniform nanoparticles. Nanoparticles were synthesized using both methods to evaluate differences in drug loading and releasing capacities. TiO_2 was chosen for its excellent biocompatibility, mechanical strength, and chemical resistance, as well as its documented anticancer activity. To prevent premature drug release, the TiO_2 nanoparticles were coated with a copolymer of Poly (methyl methacrylate) and Polyethylene glycol (PMMA-PEG), which forms a mesh-like structure that enhances drug absorption and loading capacity. The drug Resveratrol was used in this study. The synthesized nanoparticles were characterized using X-ray diffraction (XRD), ultraviolet-visible spectroscopy (UV-Vis), and scanning electron microscopy (SEM) to analyze their structural and morphological properties. These characterization results facilitated the determination of the most effective synthesis method for creating TiO_2 nanoparticles with superior anticancer activity.

Keywords: Copolymer; Drug Delivery; Hydrothermal; Sol-Gel; Resveratrol

1. Introduction

To achieve targeted drug delivery, a core-shell nanoparticle strategy was employed. Nanoparticles were chosen due to their unique chemical, physical, and biological properties at the nanoscale, which differ significantly from their properties at larger scales. This is attributed to their enhanced mechanical strength and relatively larger surface area to volume ratio, which increases reactivity [1]. Traditionally, composite nanomaterials constructed with shells (outer layer material) and cores (inner material), both at the nanoscale, are broadly defined as core-shell nanoparticles (CSNs). In this study, TiO_2 was used as the core material, and the outer layer was coated with the copolymer Poly(methyl methacrylate) and Polyethylene glycol (PMMA-PEG). Polyethylene glycol (PEG) is a well-established bio-inert and hydrophilic polymer [2,3], approved by the U.S. Food and Drug Administration (FDA) and widely used in cosmetics, drugs, and foods. Poly (methyl methacrylate) (PMMA) is another biocompatible material extensively studied and used for about 20 years as an orthopedic implant material in Europe [4]. The non-toxicity of these polymers contributed to their selection. After coating with the polymer, the nanoparticles were stable enough to hold the drug particles inside, allowing drug release only at specific pH levels. The synthesis of the core material, TiO_2 nanoparticles, can be achieved using two common approaches: (i) Top-down approach and (ii) Bottom-up approach. The top-down approach is a destructive method where bulk materials are reduced to nanoparticles, while the bottom-up approach is a constructive method where particles are built from clusters of atoms into nanoparticles [5]. In this comparative study, two synthesis methods from the bottom-up approach were used: the hydrothermal method and the sol-gel method. In both synthesis methods, particles are built up from smaller units. Among these methods, sol-gel synthesized TiO_2 nanoparticles demonstrated higher efficiency compared to those synthesized by the hydrothermal method).

2. Experimental

2.1 Synthesis of TiO_2 by Hydrothermal Method

To prepare a 0.1 N solution of Titanium tetra isopropoxide, 20 ml of ethanol was added and the mixture was stirred continuously for 30 minutes. Then, 10 ml of deionized water was introduced to form the dispersion medium. This solution was subjected to ultrasonication for 20 minutes to ensure thorough dispersion of the particles. Post-sonication, the solution was transferred to an autoclave and heated in a muffle furnace at 150 °C for 3 hours. After cooling to room temperature, the solution was washed with deionized water to remove impurities. The sample was then dried on a hotplate at 110 °C and subsequently annealed at 500 °C for 4 hours. This process yielded the

formation of TiO_2 nanoparticles [6].

2.2 Synthesis of TiO_2 by Sol-gel Method

To synthesize the nanoparticles, 10 ml of titanium isopropoxide was mixed with 30 ml of ethanol and stirred continuously for 60 minutes (referred to as Beaker 1). In a separate beaker, 3 ml of HNO_3 was added to 150 ml of deionized water to serve as a hydrolysis catalyst. This catalyst solution was then added dropwise to Beaker 1, and the resulting mixture was stirred for 2 hours at a temperature between 50 °C and 60 °C, forming a highly viscous solution. The viscous solution was then heated at 100 °C for 24 hours to allow the solvents to evaporate, leaving behind a dry compound. This dry compound was subsequently annealed for 4 hours, resulting in the formation of nanoparticles [6].

2.3 Preparation of PMMA-PEG nanoparticles

The PMMA-PEG copolymer was synthesized using the double-emulsion method, as illustrated in Figure 1. The primary emulsion was prepared by dissolving 100 mg of MMA in 1 mL of dichloromethane and adding 500 µL of hydrogen peroxide as an initiator. Separately, 20 mg of PEG was dissolved in distilled water and then combined with a PVP solution (2 mg PVP in 5 mL distilled water). The MMA solution was then added to the PEG-PVP mixture and sonicated for 2 minutes at 0 °C. To create the secondary emulsion, 20 mL of a 0.001 M sodium chloride solution containing 3% w/w PVA was added dropwise to 6 mL of the primary emulsion while stirring thoroughly. This reaction mixture was stirred for an additional 5 minutes at 0 °C. Subsequently, the solution was mixed with 1% w/w PVA solution and sonicated for 3 minutes to form the desired double emulsion. The polymer mixture was then added to a cold solution containing 10 M sodium hydroxide and 0.2 M potassium dihydrogen phosphate, made up to a total volume of 20 mL with distilled water. This solution was stirred for 30 minutes, resulting in the formation of a white precipitate. The solid was washed multiple times with distilled water and centrifuged at 5000 rpm to concentrate the PMMA-PEG nanoparticles into a fine powder. Finally, the nanoparticles were harvested and lyophilized using a Universal Lab Product Co's freeze dryer for 24 hours [7].

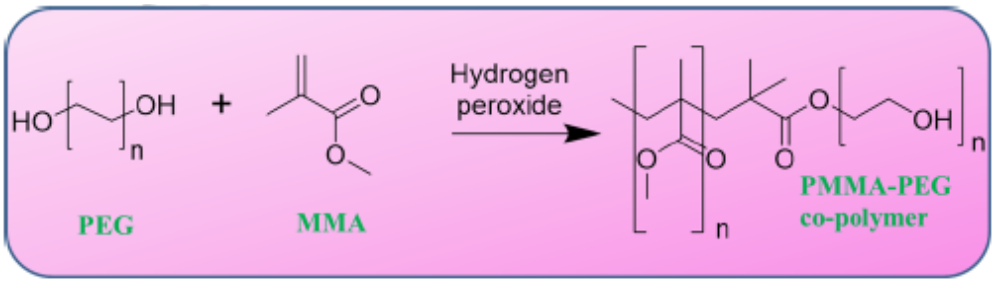

Figure 1: Synthesis of PMMA-PEG Nanoparticles

2.4 Preparation of Reveratrol loaded PMMA-PEG/TiO_2 bio nanocomposite

To prepare the resveratrol-loaded PMMA-PEG/TiO_2 nanocomposite, 100 mg of TiO_2 nanoparticles was dispersed in distilled water and sonicated for 5 minutes. Separately, PMMA-PEG nanoparticles were suspended in ethanol at a concentration of 1% w/w. The PMMA-PEG suspension was then combined with the TiO_2 solution and stirred for 24 hours at 0 °C. After this, 50 µL of TWEEN 20 was added, and the mixture was allowed to stir for an additional 2 hours. Subsequently, 100 mg of resveratrol dissolved in ethanol was added dropwise to the PMMA-PEG/TiO_2 nanoparticle suspension, and the stirring was continued for 12 hours. The resulting resveratrol-loaded solution was stored at -2 °C for 24 hours, allowing the precipitate to settle at the bottom of the vessel. The precipitate was collected by centrifugation at 4000 rpm. Finally, the solvent was evaporated using a warm water bath, concentrating the nanoprecipitate. The final product, a fine powder of resveratrol-loaded PMMA-PEG/TiO_2 nanocomposite, was obtained [8]

3. Results and Discussion

3.1 X-Ray Diffraction

The X-Ray Diffraction technique analyzed the size and purity of the nanoparticles.

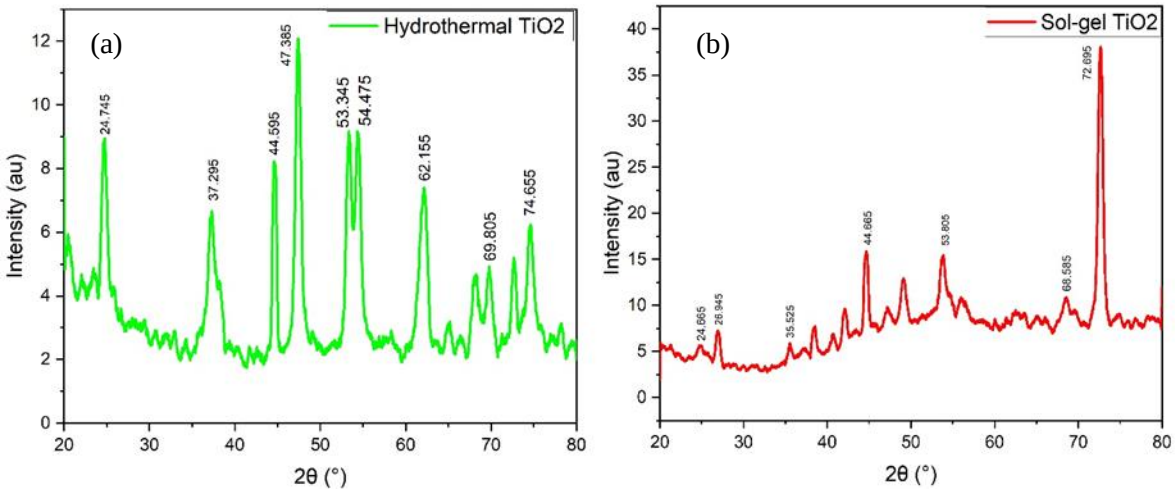

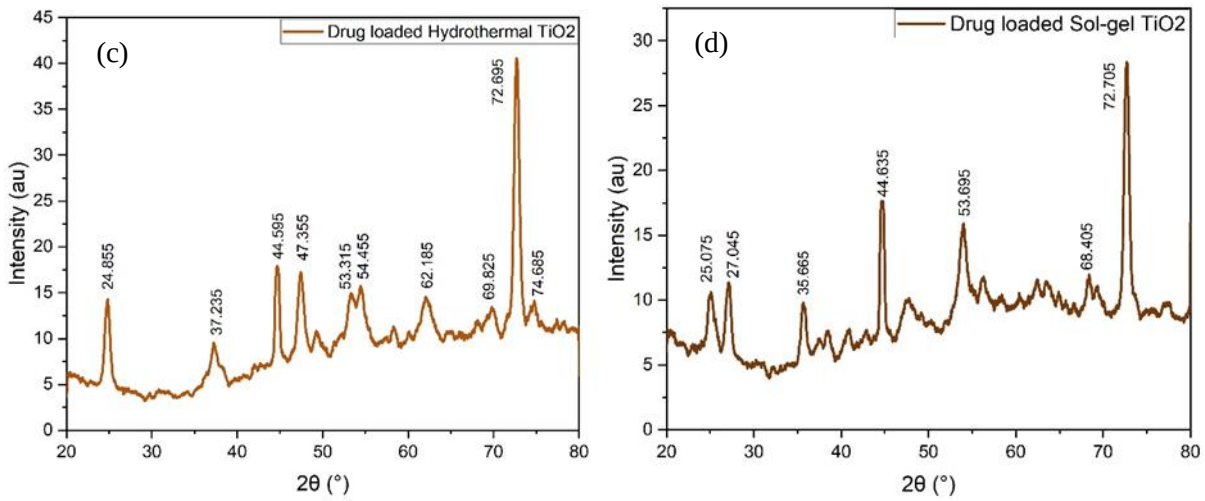

Figure 2: XRD images of (a) Hydrothermal synthesized TiO_2 nanoparticles (b) Sol-gel synthesized TiO_2 nanoparticles (c) Resveratrol loaded PMMA-PEG/TiO_2 bio nanocomposite (Hydrothermal method (d) Resveratrol loaded PMMA-PEG/TiO_2 bio nanocomposite (Sol-gel method)

Table 1: Significant 2θ Diffraction angle (°) obtained in XRD

Compounds			Significant 2θ Diffraction angle (°)		
Hydrothermal synthesized TiO_2 nanoparticles	24.745	44.595	53.345	68.105	72.635
Sol-gel synthesized TiO_2 nanoparticles	24.665	44.665	53.805	68.585	72.695
Reveratrol loaded PMMA-PEG/TiO_2 bio nanocomposite (Hydrothermal Method)	24.855	44.595	53.315	68.435	72.695
Reveratrol loaded PMMA-PEG/TiO_2 bio nanocomposite (Sol-Gel Method)	25.075	44.635	53.695	68.405	72.705

These peaks denote the crystalline structure of the drug and the metal oxide. By analyzing the peaks in the XRD obtained we have found the size of the nanoparticles formed by both the methods and calculations. Scherrer equation is used for calculating the size of the nano particles.

$$D = \frac{k\lambda}{\beta \cos \theta}$$

where D = particle size (nm),

k = 0.9 Scherrer constant,

λ = the wavelength of the X-ray (0.15406)

Table 2: Calculation for size of nanoparticles for Hydrothermal synthesized TiO_2

Peak position (2 theta)	**FWHM**		**Crystallites size D (nm)**	**Average (nm)**
23.15152	7.75537		1.045627591	10.09848222
37.37981	1.46403		5.728392466	
44.65247	0.5039		17.04323773	
47.42094	0.76905		11.28235685	
53.34582	0.73924		12.02636343	
54.42121	0.8463		10.55521043	
62.06666	1.06913		8.671831363	
68.20345	0.91419		10.49458913	
69.7586	0.88131		10.98810092	
72.68752	0.68176		14.46674982	
74.59509	1.13731		8.780844704	

From the calculations we have obtained average nanoparticles size is 10 nm for Hydrothermally synthesized TiO_2 nanoparticles.

Table 3: Calculation of size of nanoparticle for sol-gel synthesized TiO_2

Peak position (2 theta)	**FWHM**		**Crystallites size D (nm)**	**Average**
22.55071	2.42978		3.206444662	7.785373
38.43132	30.19579		0.248434781	
38.43132	0.51276		14.63001105	
42.09314	0.48499		15.28756521	
44.64854	0.50714		14.49078326	
47.54706	19.15298		0.379585022	
53.85403	0.9593		7.383510713	
68.65935	1.28553		5.103299078	
72.65215	0.68536		9.338721502	

The calculations we have obtained average nanoparticles size is 7 nm for Hydrothermally synthesized TiO_2 nanoparticles.

3.2 Diffuse Reflectance Spectroscopy

The optical properties of the TiO_2 nanoparticles were examined through Diffuse Reflectance Spectroscopy (DRS). Below is the UV–Visible reflectance spectrum of the TiO_2 nanoparticles. The spectra obtained at 385 nm reveal the charge-coordinated electronic transition between the O 2p state and Ti at the 3d state [9]. The distinct absorption peak indicates a shift in the crystalline phase and average crystalline size, affirming the suitability of the investigated nanomaterial for catalytic applications. Additionally, the pronounced absorbance peak within the 335–380 nm region provides further evidence of TiO_2 NP formation [10]

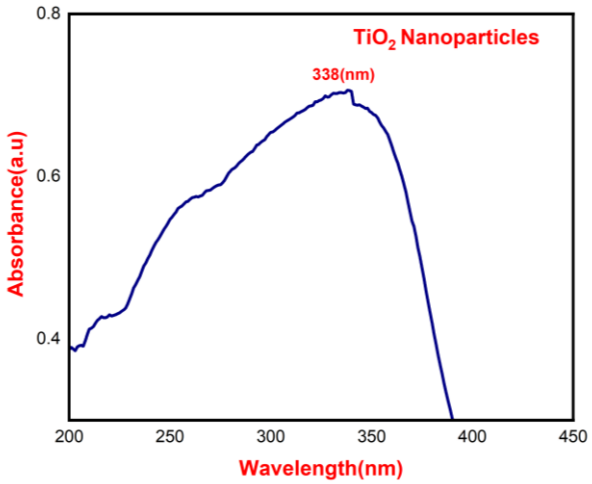

Figure 3: DRS graph of the TiO_2 Nanoparticles

3.3 Scanning Electron Microscopy

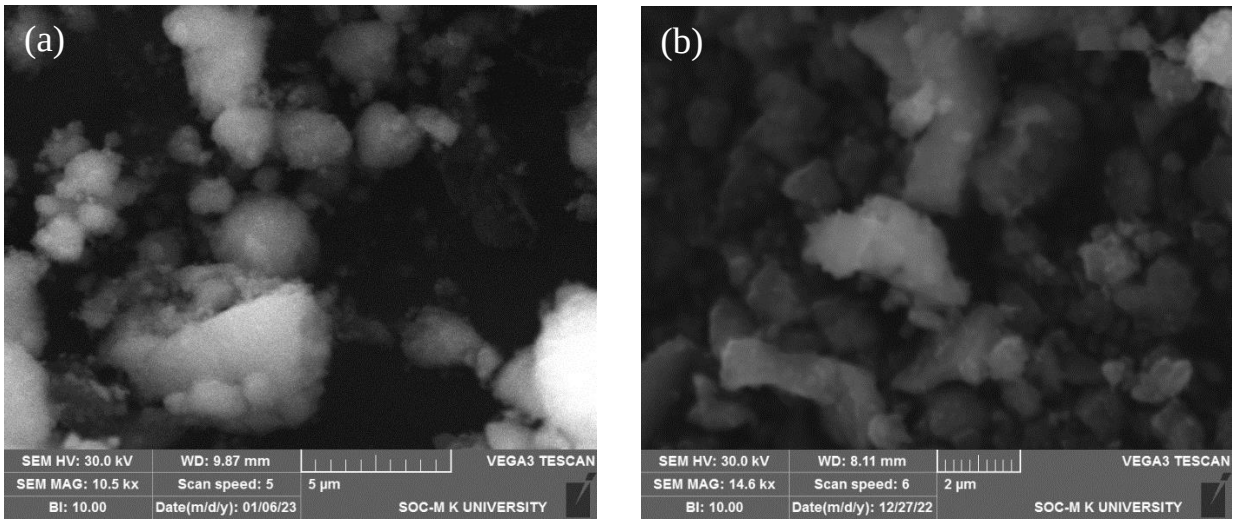

Figure 4: Micrograph images of (a) Hydrothermally synthesized TiO_2 NPs and (b) Sol-gel synthesized TiO_2 NPs

SEM images revealed sphere-like surface shapes of TiO_2 nanoparticles, with an average particle size falling within the range of 5-10 nm. The particle size determined via SEM correlates closely with the average crystalline size determined through XRD analysis. Generally, the reduction in particle size is inversely related to the material's surface volume. Consequently, materials with smaller particle sizes exhibit enhanced penetration capabilities, facilitating the breakdown process of toxic substances and bacterial surfaces.

3.4 Antibacterial Activity

In the following paragraph consider nanoparticles I as Hydrothermal synthesized TiO_2 loaded with drug & Nanoparticle II is Sol-gel synthesized TiO_2 loaded with drug.

3.4.1 Well diffusion assay

Nanoparticles I and II were assessed for their antibacterial activity against five distinct human pathogenic microorganisms: Bacillus subtilis and Staphylococcus aureus (Gram-positive), and Escherichia coli, Pseudomonas aeruginosa, and Salmonella typhi (Gram-negative) using the well diffusion method. The test microorganisms were evenly spread on nutrient agar (NA) petri plates. Wells were then created on the agar plates using a cork borer, followed by the addition of varying concentrations (100 and 200 µg/ml) of nanomaterials into the wells, along with positive (streptomycin) and negative (DMSO) controls. The plates were subsequently incubated for 24 hours at 37°C, and the zones of inhibition were observed and recorded. The mean of three replicates was utilized to analyse the outcomes [11].

3.4.2 Antibacterial activity

Nanoparticles I and II exhibit notable antibacterial activity against five human pathogenic microorganisms, namely E. coli, S. typhi, P. aeruginosa, B. subtilis, and S. aureus, as determined by the well diffusion method. The zones of inhibition for the nanomaterials ranged from 8.00±1.00 mm to 23.66±1.15 mm. Notably, Nanoparticle II demonstrates superior efficacy against E. coli and B. subtilis, with inhibition zones measuring 22.33±1.52 mm and 23.66±1.15 mm, respectively, at a concentration of 200 µg/ml, compared to other pathogenic bacteria. Conversely, Nanoparticle I exhibit lower activity, with inhibition zones averaging 8.00±1.00 mm. Streptomycin sulphate, utilized as a control, displays inhibition zones ranging from 24.33±1.15 mm to 33.33±1.52 mm at a concentration of 50 µg/ml. The measurement data for the zones of inhibition are presented in Table 4.

Table 4: The zone of inhibition

S. No	Test compounds	Concentrations (µg/ml)	Zone of inhibition in (mm)				
			Gram negative microorganisms			Gram positive microorganisms	
			E. coli **(ATCC 3739)**	***S. typhi*** **(MTCC 733)**	***P. Aeruginosa*** **(ATCC27853)**	***B. subtilis*** **(ATCC 11774)**	***S. aureus*** **(ATCC 6518)**
1	I	100	09.36±1.48	10.31±0.49	10.31±0.51	07.80±1.00	08.26±1.05
		200	10.00±1.00	11.00±1.00	11.00±1.53	10.00±1.00	12.13±1.12
3	II	100	14.48±1.51	11.00±1.00	12.18±0.53	18.76±1.52	12.21±1.42
		200	23.26±1.15	14.83±1.52	13.10±1.00	20.52±1.52	15.24±1.15
4	Streptomycin sulphate (+Ve)	50	32.23±1.52	23.93±1.15	23.99±1.52	30.23±1.15	26.70±1.63
5	DMSO (-Ve)	50	-	-	-	-	-

3.5 Minimum Inhibition Concentration

Nanomaterials I and II underwent a micro-dilution procedure to determine their minimal inhibitory concentration (MIC). This method, employing a color scoring scheme, revealed MIC values after 24 hours of treatment with the nanomaterials. The microorganisms were exposed to nanomaterials at concentrations ranging from 500 µg/ml to 3.90 µg/ml. The minimum inhibitory effect was observed within the concentration range of 3.90 - 125 µg/ml. Sample II exhibited an inhibitory effect range of 3.89–61.9 µg/ml, whereas Sample I showed an inhibitory effect range of 29.25–119 µg/ml. Notably, Sample II demonstrated superior inhibitory activity against P. aeruginosa, S. typhi, and E. coli, with MIC values of 3.79 µg/ml, 7.64 µg/ml, and 7.73 µg/ml, respectively. Specifically, Sample II exhibited remarkable effectiveness, with a MIC value of 3.82 µg/ml against P. aeruginosa, compared to the other four pathogenic bacteria. Overall, nanomaterial II displayed greater efficacy than nanomaterial I (see Table 5). Streptomycin served as the positive control in this study, while DMSO served as the negative control, demonstrating no inhibition. These findings suggest the potential utility of these nanomaterials as antimicrobial agents in future applications.

Table 5: Minimum inhibitory concentration (MIC) of nanomaterials against human pathogenic microorganisms using by micro dilution method

S. No	Test compounds	MIC (µg/ml)				
		Gram negative microorganisms			Gram positive microorganisms	
		E. coli **(ATCC 3739)**	***S. typhi*** **(MTCC 733)**	***P. Aeruginosa*** **(ATCC27853)**	***B. subtilis*** **(ATCC 11774)**	***S. aureus*** **(ATCC 6518)**
1	I	31.08	61.5	29.25	131.0	131.0
2	II	7.61	7.71	3.87	31.28	15.42
4	Streptomycin sulphate (+Ve)	7.61	15.42	31.25	15.57	7.79
5	DMSO (-Ve)	-	-	-	-	-

4. Conclusion

Here, we have performed a thorough investigation of the characteristics and performance of TiO_2 nanoparticles developed using two different processes such as, sol-gel (SG) and the hydrothermal (HT) approaches. This study revealed an important information on the subtle differences between the two synthesis methods. Although TiO_2 nanoparticles were successfully produced using both methods, our careful examination revealed that the sol-gel could develop more efficient TiO_2 nanoparticles than the hydrothermally synthesized materials in exhibiting strong antibacterial activity. Interestingly, our results highlight the sol-gel method as a model of ease of use and economy in the fabrication of nanoparticles. Moreover, this approach has significant implications for the advancement of tailored drug delivery systems at a relatively low cost in addition to providing a simplified and financially feasible method of synthesizing nanoparticles. Through the refinement and expansion of the sol-gel methodology, we envision a novel path in biomedical engineering, where therapeutic interventions are revolutionized and improved accessibility and efficacy of healthcare are made possible through the seamless integration of state-of-the-art technology and affordable solutions.

Conflicts of interest

The authors declare that they have no conflict of interest.

References

1. R. Kumar, K. Mondal, P.K. Panda, A. Kaushik, R. Abolhassani, R. Ahuja, H.-G. Rubahn, Y.K.

Mishra, Core-shell nanostructures: perspectives towards drug delivery applications, J Mater Chem B (2020). https://doi.org/10.1039/d0tb01559h.

2. R. Hayes, A. Ahmed, T. Edge, H. Zhang, Core–shell particles: Preparation, fundamentals and applications in high performance liquid chromatography, Journal of Chromatography A 1357 (2014) 36–52. https://doi.org/10.1016/j.chroma.2014.05.010.
3. F.M. Galogahi, Y. Zhu, H. An, N.-T. Nguyen, Core-shell microparticles: Generation approaches and applications, Journal of Science: Advanced Materials and Devices 5 (2020) 417–435. https://doi.org/10.1016/j.jsamd.2020.09.001.
4. C. for D.E. and Research, Novel Drug Approvals for 2024, FDA (2024). https://www.fda.gov/drugs/novel-drug-approvals-fda/novel-drug-approvals-2024 (accessed May 23, 2024).
5. P.G. Jamkhande, N.W. Ghule, A.H. Bamer, M.G. Kalaskar, Metal nanoparticles synthesis: An overview on methods of preparation, advantages and disadvantages, and applications, Journal of Drug Delivery Science and Technology 53 (2019) 101174. https://doi.org/10.1016/j.jddst.2019.101174.
6. R. Dhivya, J. Ranjani, P.K. Bowen, J. Rajendhran, J. Mayandi, J. Annaraj, Biocompatible curcumin loaded PMMA-PEG/ZnO nanocomposite induce apoptosis and cytotoxicity in human gastric cancer cells, Materials Science and Engineering: C 80 (2017) 59–68. https://doi.org/10.1016/j.msec.2017.05.128.
7. J. Avossa, G. Herwig, C. Toncelli, F. Itel, R.M. Rossi, Electrospinning based on benign solvents: current definitions, implications and strategies, Green Chem. 24 (2022) 2347–2375. https://doi.org/10.1039/D1GC04252A.
8. J. Roy, The synthesis and applications of TiO2 nanoparticles derived from phytochemical sources, Journal of Industrial and Engineering Chemistry 106 (2022) 1–19. https://doi.org/10.1016/j.jiec.2021.10.024.
9. M. Aravind, M. Amalanathan, M.S.M. Mary, Synthesis of TiO2 nanoparticles by chemical and green synthesis methods and their multifaceted properties, SN Appl. Sci. 3 (2021) 409. https://doi.org/10.1007/s42452-021-04281-5.
10. D. Ziental, B. Czarczynska-Goslinska, D.T. Mlynarczyk, A. Glowacka-Sobotta, B. Stanisz, T. Goslinski, L. Sobotta, Titanium Dioxide Nanoparticles: Prospects and Applications in Medicine, Nanomaterials (Basel) 10 (2020) 387. https://doi.org/10.3390/nano10020387.
11. E. Urnukhsaikhan, B.-E. Bold, A. Gunbileg, N. Sukhbaatar, T. Mishig-Ochir, Antibacterial activity and characteristics of silver nanoparticles biosynthesized from Carduus crispus, Sci Rep 11 (2021)

21047. https://doi.org/10.1038/s41598-021-00520-2.